

Multiple-Beam Low-Profile Low-Cost Antenna

Paul G. Elliot, Kiersten C. Kerby-Patel, Drayton L. Hanna,
The MITRE Corporation
202 Burlington Road, Bedford, MA 01720
pelliott@mitre.org ph: 781-271-3477 fax: 781-271-4691

Introduction

Low-cost directional antennas with electronic beam agility are a high priority requirement for many systems. This paper describes an antenna built and tested in June 2012 which provides multiple low elevation angle beams around the full 360 degrees in azimuth, and is low-height and low-cost (patent pending).

The antenna design objectives were:

- Coverage of all azimuth angles (360°) using multiple beams.
- Rapid electronic beam switching between beams.
- Maximize gain coverage over 5° to 35° elevation for each beam.
- Frequency: X/Ku-band 8.2 – 12.2 GHz
- Vertical linear polarization.
- Minimize Size, Weight, Power, and Cost (SWaP-C) of antenna and electronics.
- Provide the above performance with no external ground plane, or on a very small ground plane.

Elevation scan was not required; the multiple beams are distributed around azimuth at a fixed elevation angle. The antenna diameter including ground plane and radome was 6.156" (156.4 mm), which is 5.2 wavelengths at 10 GHz, no other ground plane was used. The measured boresight gain for all the beams was about 15 dBi, with the beam maximum located at 24 degrees elevation, and very wideband. The gain at the beam cross-over angles (between beams in azimuth) is about 1½ dBi lower than the boresight gain. The height of the antenna and radome above the ground plane is 0.961" (24.4 mm) which is 0.8 wavelengths at 10 GHz; this is the distance it would protrude into the airstream when installed on a platform.

An earlier prototype was reported by the same authors in 2010 [1][2]. The 2010 design used an infinite ground plane for the computer model to reduce computer run time, but as a result the design was suboptimal for a small size ground plane. Placing the antenna on a finite size ground plane limits the

achievable gain for low-angle beams due to diffraction and creeping waves over the edge of the ground plane, which widens the beam in the elevation plane near the horizon. This was observed in measurements on rolled-edge ground planes as large as 51" diameter. Therefore, for best computer modeling accuracy, the finite ground plane should be included in the computer model. This was done in 2012 and the antenna was designed to use a 6" (156 mm) diameter ground plane, and other dimensions reoptimized to improve performance. A radome was added for the 2012 design and tests.

Antenna Description and Photos

Figure 2.1-1 shows a photo of the June 2012 antenna with the radome removed. The dark circle on the top is Duroid material, the white is Rohacell foam which secures the other parts in place. A small aluminum ground plane and an aluminum rim are seen around the bottom of the antenna; this antenna was designed to work well with the 6.156" (156.4 mm) diameter ground plane which is incorporated into the antenna structure.

Figure 2.1-2 is a photo of the back side of the 6" wide ground plane showing the 27 feed port SMA coaxial connectors in a circle near the periphery. Switching between beams is accomplished by switching between the 27 feed ports. The resulting 27 beams are spaced around azimuth with angular beam separation of $360^\circ/27 = 13.33^\circ$. Each SMA connector drives a small brass feed monocone which launches the wave into the lens and radiates a beam at low elevation on the opposite side from the driven feed port. Figure 2.1-3 shows a cross-sectional drawing of the antenna.

The dielectric parts have no metallization except a layer of small etched copper circular discs on the Duroid slab seen in Figures 2.1-1 and 2.1-3, which provides a partially reflective upper surface, producing a leaky-wave between the dielectric top layers and the 6" ground plane [1], the leaky wave radiates from the top surface of the antenna. The Duroid cone helps focus and collimate the energy into the forward beam direction. The power handling

capability of the antenna is determined by the SMA connectors in Figure 2.1-2 and by the external electronics such as switch matrix.

Figure 2.1-4 shows the antenna on a mounting fixture. Figures 2.1-5 shows the radome placed over the antenna and mounting fixture. The radome covers the antenna and also the volume behind the antenna to protect the electronics from rain or snow which might be wafted into the bay surrounding the antenna.

Measured Antenna Performance

For these measurements the antenna included the built-in 6" ground plane and the radome, no other ground plane or amplification was used for these measurements. The patterns shown are for a single port transmitting, the patterns of each other port should be practically identical (just rotated in azimuth) due to the circular symmetry of the antenna. The elevation coverage is the same for all beams; the beam is not switchable or scanned in elevation.

For these measurements the remaining 26 unused ports seen in Figure 2.1-2 were either terminated with a 50-ohm load, or were connected to very short lengths of open-circuited ("OC") coax ($\frac{1}{4} \lambda$ long at 10 GHz) to produce a short-circuit at the lens ground plane, which reflects the power back into the lens with a beneficial phase for increasing gain. These two terminating conditions are labeled in the legends or titles of most pattern plots: red curves used the 50 ohm loads; blue curves used the OC coaxes.

The θ, ϕ pattern angles refer to a spherical coordinate system. For these tests the antenna was facing upwards so the Z axis ($\theta=0^\circ$) is towards zenith. The 6" wide ground plane is parallel to the horizon or azimuth plane which is the XY plane: $\theta=\pm 90^\circ$. The antenna radiates vertical polarization (E_θ), which is the polarization plotted in the patterns in dBi. The dBi scale on the free-space plots is -20 to +20 dBi with 10 dBi grid circles.

Figure 2.2-1 shows the measured elevation pattern cut at 10 GHz. The main lobe maximum is +14.8 dBi (blue curve) and +14.4 dBi (red curve) at an elevation angle of 24° above the horizon (elevation angle is $90^\circ - \theta$ on right of the plot, or $\theta - 270^\circ$ on left of plot). The blue curve shows half-power beamwidth (HPBW) coverage in elevation from 3° up to 36° which gives a 33° HPBW. The red curve shows HPBW in elevation from 4° up to 37° which gives a 33° HPBW.

Figure 2.2-2 shows the azimuth cut around 360° at the horizon, which has gain of 11.2 dBi (blue) and 10.2 dBi (red) which is lower than the main lobe peak gain since the main lobe is above the horizon. The HPBW is 18° . Figure 2.2-3 shows a conical cut around 360° azimuth through the main lobe peak, so the elevation angle stays constant at 24° ; the HPBW is 20° (blue) or 18° (red). The beam shape is therefore somewhat of a "fan" beam since the elevation beamwidth is much wider than the azimuth beamwidth. The highest sidelobes in these azimuth and conical cuts are seen to be about 10 dB below the main lobe, and the backlobes are about 20 dB below the main lobe peak. These side and back lobe levels are much improved over earlier prototypes [1]. 27 beams spaced around azimuth produce angular beam separation of $360^\circ/27 = 13.33^\circ$ for this antenna, resulting in beam crossover levels in azimuth of about 1.5 dB down from the maximum in each cut.

Figures 2.2-4 through 2.2-7 show that the antenna covers extremely wide instantaneous bandwidths: Figures 2.2-4 and 2.2-5 overlay the elevation cuts at numerous frequencies in 0.2 GHz steps, which show that the main beam pattern coverage is maintained over very wide bandwidths. Figure 2.2-6 plots the gain vs. frequency at the gain maximum and at the horizon. It is also seen in Figures 2.2-4 through 2.2-6 that a wider frequency bandwidth is obtained by using the 50 ohm terminations on the unused ports (red curve), while a slightly higher gain from 9 to 11 GHz is obtained by using the OC coax on the unused ports.

The S-parameters of the antenna ports were also tested using a network analyzer. Figure 2.2-7 plots the measured return loss (S_{11}) for a sample port. The S_{11} impedance bandwidth is seen to be widest for the 50- Ω terminated case, as was also seen for the gain bandwidth in Figures 2.2-4 through 2.2-6. Figure 2.2-8 plots the mutual coupling (S_{n1}) to all the other ports, it is seen to be very low (< -20 dB) to all the ports except the two closest ports are about -16 dB.

The measured crosspolarization level (E_ϕ) was -25 dB below the copolarized main lobe in the elevation plane, -22 dB in the azimuth horizon plane, -13 dB in the conical cut at 24° elevation, and -13 dB was also the highest crosspole level in the entire pattern. These levels are with the OC coax on unused ports, the crosspole levels are up to 2 dB higher if using 50 Ω terminations.

Computed Antenna Patterns

Prior to fabrication, the antenna design was computer modeled and optimized using High Frequency Structure Simulator (HFSS) electromagnetic software from Ansys Corporation, with the Distributed Solve Option to speed the optimizations. The 6" wide ground plane and the radome were included in these simulations. The optimization goals used in HFSS were the objectives outlined in the Introduction, primarily at 10 GHz to maximize the mean realized gain over the fan beam region, including gain at the beam crossovers.

The resulting computed patterns at 10 GHz are shown in Figures 2.4-1 through 2.4-3. The HFSS computer simulation used the OC, not the 50-ohm terminations, on the 26 undriven ports. These computed patterns are in good agreement with the measured patterns with OC terminations (blue curves) shown in the preceding Section, including the main lobe, sidelobes, and backlobes. The computed maximum gain at 10 GHz is 16 dBi. The agreement with the measured maximum gain and horizon gain is within 1 to 2dB. This accuracy can be typically obtained when the finite ground plane is included in the HFSS computer model. The agreement with the measured patterns was less good below 9 GHz and above 11 GHz, probably due mainly to approximations in the way the OC coax was computer modeled.

Antenna Electronics Options for Beam Selection

The azimuth beam direction would be selected by switching to one of the port connectors shown in Figure 2.1-2. For the measurements so far this has been connected manually. A switch matrix could be used so the beam ports would be selected under computer control. For example, a SP27T switch matrix could be assembled by using 3 levels of SP3T since $3 \times 3 \times 3 = 27$ outputs. In that case, one port would be transmitting and receiving at any given time.

The OC coax fixtures used on the unused ports provides higher antenna gain near 10 GHz but less bandwidth than the 50-ohm terminations; this was seen in the patterns and in reference [1]. It is also less expensive and lighter-weight to make a switch matrix with OC than 50-ohm terminations. However, the length of coax from the antenna input to the OC is short in length since it must be $\frac{1}{4} \lambda$ at 10 GHz (or another multiple of $\frac{1}{4} \lambda$ although that would reduce bandwidth), so the switch layout must be carefully planned so the switch ports are close enough to the antenna ports.

Using a more elaborate switch matrix, or with a signal synthesizer and/or digital beamformer at each port it would be possible, in principle, to combine beams and/or to transmit and receive from multiple beam directions simultaneously.

Comparison with Other Antenna Types

The novel low-profile antenna described in this report radiates from the surface of the beamforming lens; this combines a planar beamformer and radiating aperture in one lens structure. It does not need external radiating elements nor a large vertical aperture to produce multiple low-angle beams distributed 360° around azimuth. These unique features reduce the size, weight, and cost compared to other antennas with electronically switched 360° coverage such as phased arrays, 3D Luneburg lens [3], single-K spherical lens [4], and 2D Luneburg lens [5][6].

Directional antennas for SHF and EHF communications and radar systems are usually reflectors, horns, arrays, or fixed-beam lower-gain antennas. Major limitations of reflectors include increased platform height, visibility, and wind drag for a moving platform. Moreover, a reflector antenna can only illuminate one direction at a time, limiting beam steering speed and the number of simultaneous beams. Accurate mechanical pointing of the reflector is slow and reduces the ability to operate on-the-move; this lack of beam agility can result in loss of signal when the platform turns, rolls, or pitches. Many of these limitations also affect horn antennas: they are not low profile and require mechanical pointing. Another existing antenna is a fixed-beam array which is mechanically steered; it has the same basic limitations as other fixed-beam antennas such as a dish or horn.

Another directional antenna is a phased array with electronic scan. However phased arrays are expensive to design and manufacture due to the large number of radiating elements, phase shifters or T/R modules each with expensive semiconductor devices, complicated feed network, support structure, and non-recurring engineering (NRE) costs. Cost is the main reason phased arrays are not more widely used for communications applications; radar systems are more likely to use a phased array than a communications system. At Ku-band and higher it also becomes increasingly difficult to package all the components behind each array element. The frequency bandwidth of many phased arrays is limited due to mutual coupling since wideband array

elements are more expensive to design and manufacture. The number of simultaneous beam directions is typically very limited for phased arrays. Weight can be an issue for larger phased arrays, especially if they include transmit capability with cooling. A limitation for low-profile phased arrays is the difficulty in scanning the beam to low elevation angles over 360° in azimuth with wide bandwidth. If the phased array has some height, such as a cylindrical or pyramidal phased array, then low angle coverage is facilitated, but the height and wind-loading increase.

Existing 3D lens antennas have significant height such as dome-shaped [3][4]. Existing 2D lens antennas require an external aperture or radiating elements to reduce the elevation beamwidth [5][6]. The main difference between this new lens antenna and a 2D Luneburg lens [5][6] is that a 2D Luneburg lens is not designed to collimate or radiate from the lens top surface, whereas this new lens antenna radiates from the entire surface of the lens. A 2D Luneburg lens is designed to collimate only in the same plane as the lens, and therefore is usually used as beamformer feeding columns of a cylindrical array.

One existing paper [6] describes a 2D Luneburg lens which radiates from the rim of the lens without external radiating elements, but since the rim is low height and the Luneburg lens does not radiate from the lens top surface, it resulted in an extremely wide elevation beamwidth. It also did not provide full 360° coverage, and since the feed patches were only on one side of the lens, the additional feed patches required for 360° azimuth coverage might interfere with the pattern. Also the authors of [6] recommend keeping that lens about one wavelength from any metal surface, which would effectively increase the height considerably for that antenna on a fuselage or other conducting platform.

Table I provides a very brief comparison of several types of antennas which can provide a low-angle directional beam. The antenna sizes and performance were estimated by simulation. All the antennas have the same HPBWs at low elevation angles at 10 GHz, to obtain an “apples to apples” comparison. The “Max Gain” column was estimated for low angles using typical loss for that antenna. The two lens antennas (2nd and 3rd rows) would have about 1½ dB lower gain at the azimuth beam crossover angles since these use fixed multiple beam directions resulting in a gain “scallop” around azimuth. For all the other cases this loss does not occur due to the much finer resolution in azimuth beam pointing (mechanical or electronic). All these antennas can be designed for wide frequency bandwidth, except possibly the last row, which is a flat circular “Horizontal Planar Phased Array” phased for low-angle beams and scanned in azimuth and elevation, it has low height but needs a large diameter to produce the desired elevation HPBW at low elevation scan angles.

Conclusion

The new multiple-beam lens antenna described in this report offers electronic beam switching of multiple beams in azimuth over a full 360° degrees; extremely wide bandwidth; low height, weight, and cost; and also provides many of the advantages of existing directional antennas for low elevation angle coverage. The antenna diameter including ground plane and radome was 5.2 wavelengths; no other ground plane was used. The measured boresight gain for all the beams was about 15 dBi, with the beam maximum located at 24 degrees elevation. However, the new lens antenna also has disadvantages for some applications. The gain of the new lens antenna designs cannot be increased by simply increasing the size of the antenna; it has not yet exceeded about 18 dBi. Also, it does not scan in elevation, and the sidelobes are higher than for most other types of directional antennas.

Table I. Comparison of Antennas Designed for a Low-Angle Beam, with Elevation HPBW of 33° and Azimuth HPBW of 20° at 10 GHz.

Antenna Type	Electronic Scan	Diam	Height	Directivity D_0	Max Gain Estim	# Elem or # Ports
One Horn 6" long, vertically polarized	None	4.8"	1.85"	16.6 dBi	16.5 dBi	1
June 2012 Lens: described in this paper	Azimuth only	6.2"	0.96"	16.2 dBi	14.8 dBi	27
May 2012 Lens: lower height version	Azimuth only	6.2"	0.43"	14.1 dBi	12.7 dBi	27
Near-Vertical Planar Array, rotate in Az	Elevation only	3.0"	1.85"	17.0 dBi	14.0 dBi	6
Cylindrical or Pyramidal Phased Array	Azim and Elev	3.5"	1.85"	17.8 dBi	14.8 dBi	36
Horizontal Planar Phased Array	Azim and Elev	16"	<0.4"	16.9 dBi	13.9 dBi	≈600

ACKNOWLEDGEMENTS

We thank Dana Whitmer and Eddie Rosario of MITRE for antenna fabrication and measurement, respectively.

Index Terms - *Multiple Beam Antenna, Multibeam Antenna, Beamforming, Beam Forming, Beamformer, Lens Antenna, Beam Scanning, Luneburg Lens, Luneberg Lens, Smart antenna, Antenna Array, WIMAX antenna, X-Band, Ku-Band, Ka-band, EHF antenna.*

REFERENCES

[1] P. Elliot and K.C. Kerby Patel, November 1-3, 2010 "Multiple-Beam Planar Lens Antenna Prototype," *7th IASTED International Conference on Antennas, Radar, and Wave Propagation, ARP 2010*, Cambridge, Massachusetts, USA. (This paper is also included as an appendix in reference [2] below).

[2] P. Elliot, D.L. Hanna, K.C. Kerby Patel, and E.N. Rosario, "Update on X/Ku-Band Multiple-Beam Low-Profile Lens Antenna Prototypes" , MITRE Product MP120042. January 2012.

[3] John Sanford and Hal Schrank, "A Luneburg-Lens Update", *IEEE Antennas and Propagation Magazine*, vol. 37, No. 1, Feb. 1995.

[4] N. Herscovici and Z. Sipus, "A Spherical Multibeam Antenna", *IEEE Antennas and Propagation Symp.*, June 2003. vol.3 pp.693-696.

[5] Carl Pfeiffer and Anthony Grbic, "A 2D Broadband Printed Luneburg Lens Antenna", *IEEE Antennas and Propagation Society Intl Symposium*, 2009. June 2009, Charleston SC. USA. pp 1-4.

[6] L. Xue and V. Fusco, "Patch-fed Planar Dielectric Slab Waveguide Luneburg Lens", *Microwaves, Antennas & Propagation, IET*, March 2008. Volume 2, Issue 2, pp 109 -114.

FIGURES

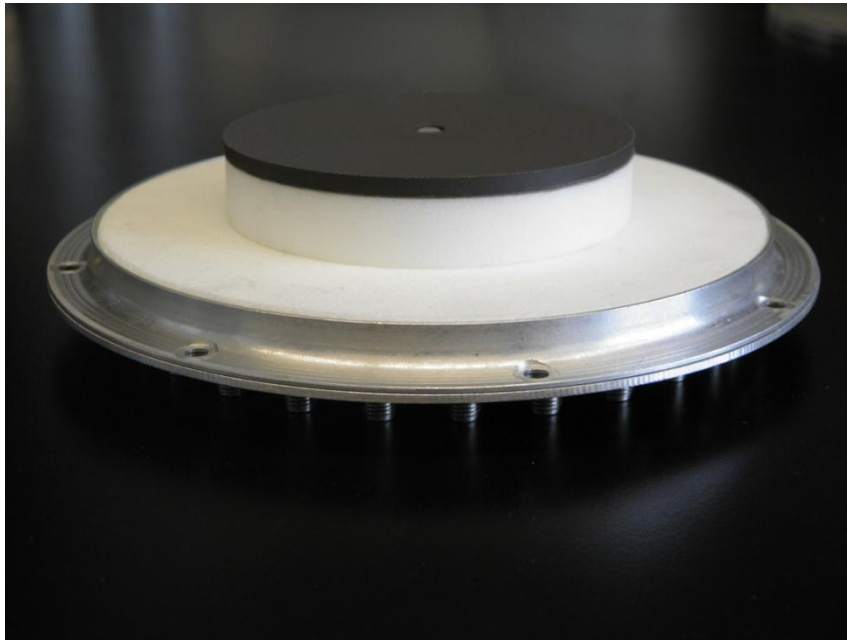


Figure 2.1-1. Close up View of Antenna with Radome removed.

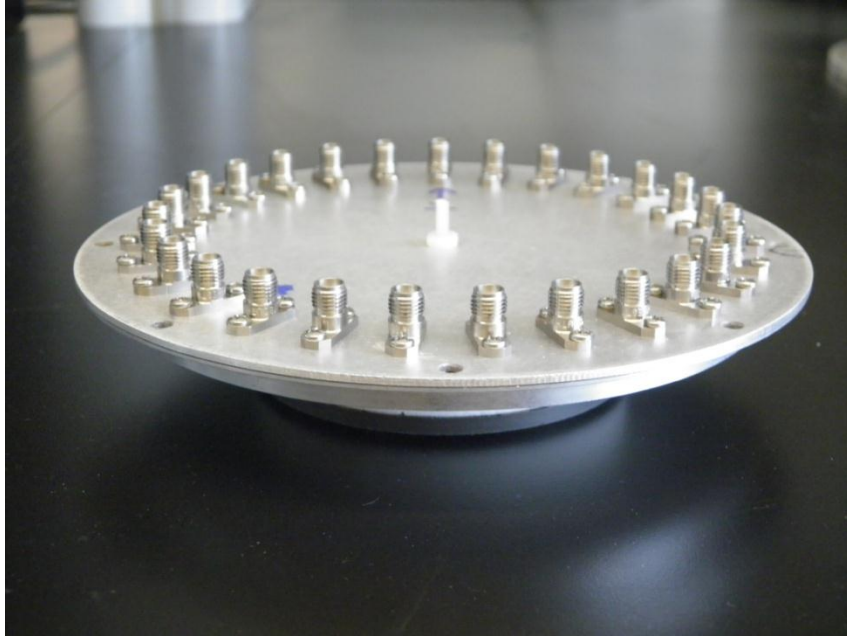


Figure 2.1-2. Rear of Ground Plane showing the 27 Feed Port Coaxial Connectors.

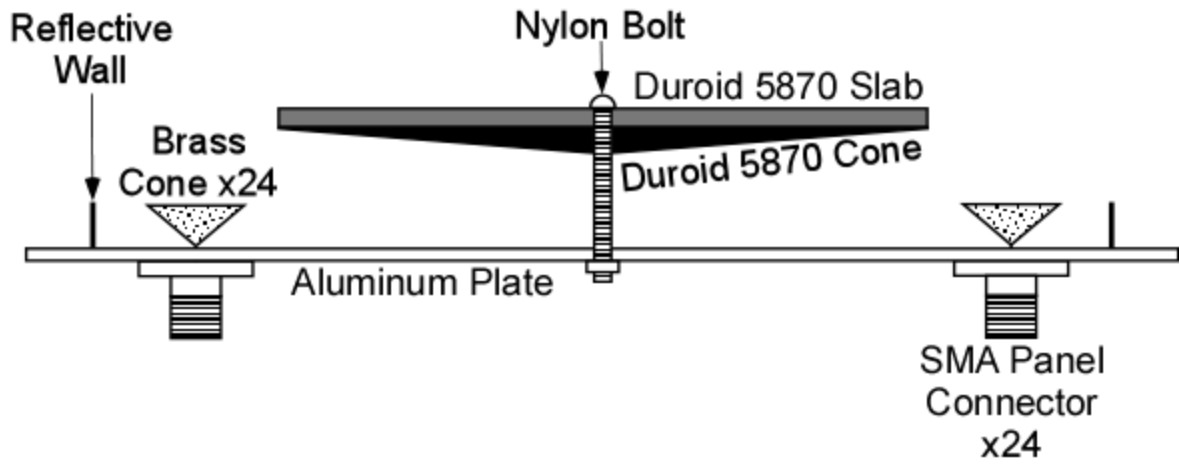


Figure 2.1-3: Cross-Sectional Side View Drawing of Antenna (Radome and Foam not shown).

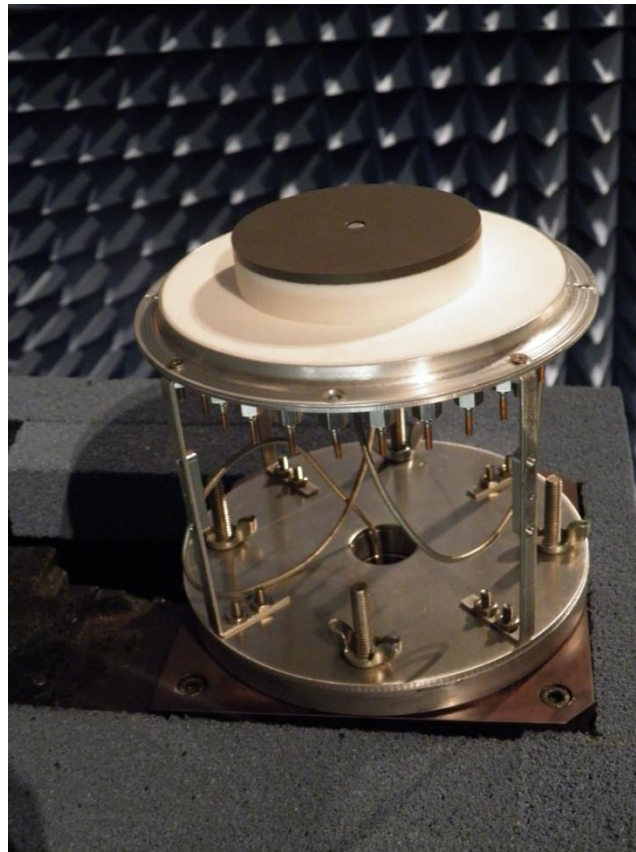


Figure 2.1-4. Antenna on Mounting Fixture.



Figure 2.1-5. Radome placed over the Antenna and Mounting Fixture.
The Antenna occupies only the Top 1" of the Radome.

Far-field amplitude of DSPH12170a1.NSI

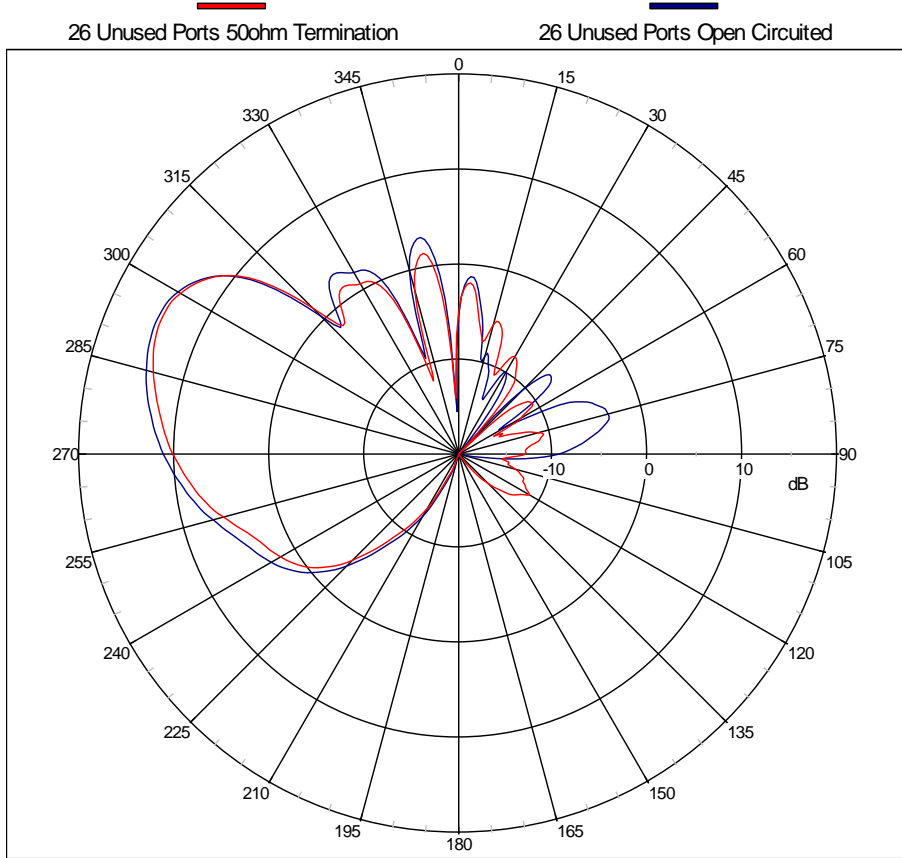


Figure 2.2-1. Measured Elevation Pattern Cut at 10 GHz. The pattern maximum is at 24° Elevation.

Far-field amplitude of DSPH12170a1.NSI

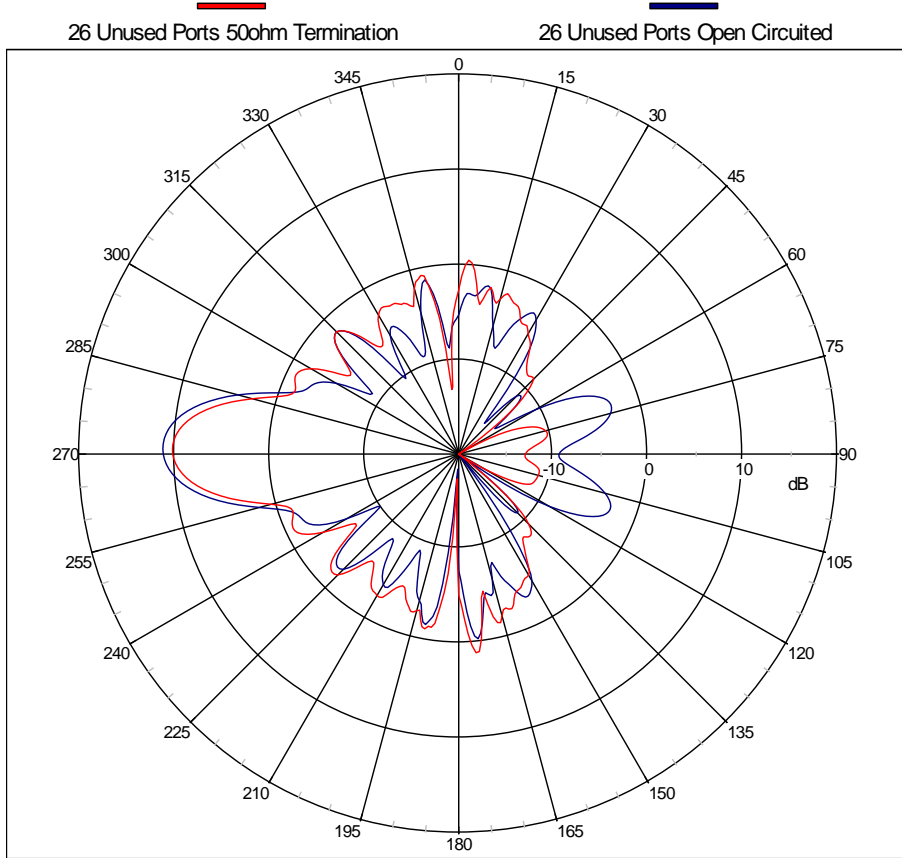


Figure 2.2-2. Measured Azimuth (Horizon) Pattern Cut at 10 GHz.

Far-field amplitude of DSPH12170a1.NSI

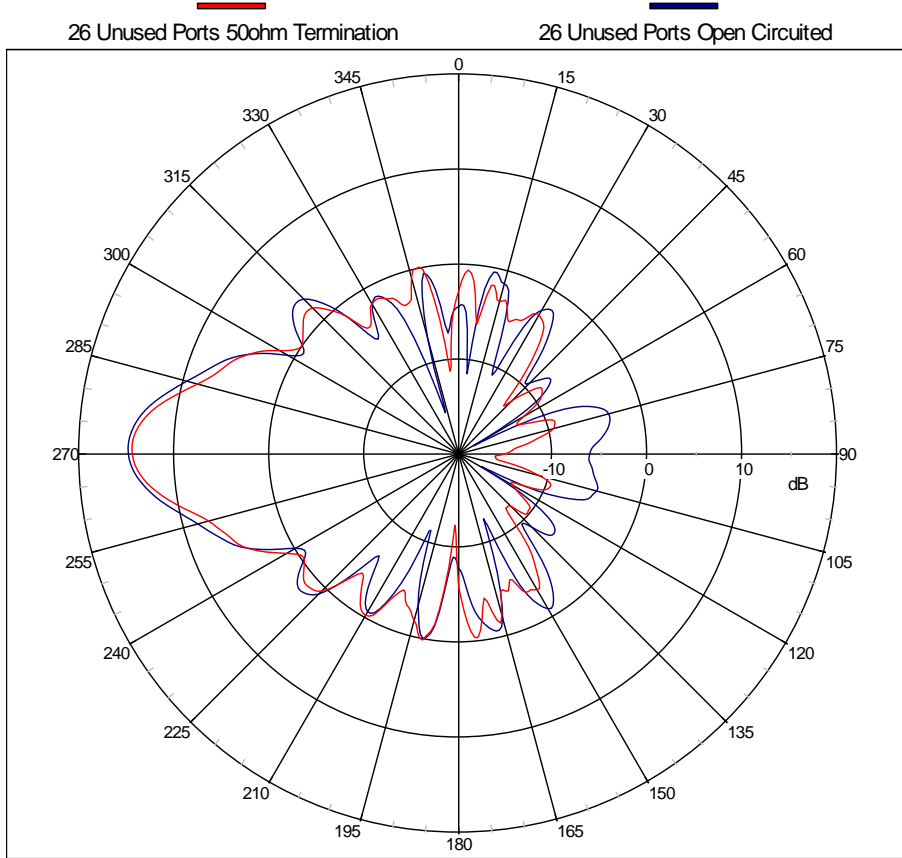


Figure 2.2-3. Measured Conical Pattern Cut around all Azimuths at 26° Elevation (i.e. passes through main lobe peak), at 10 GHz.

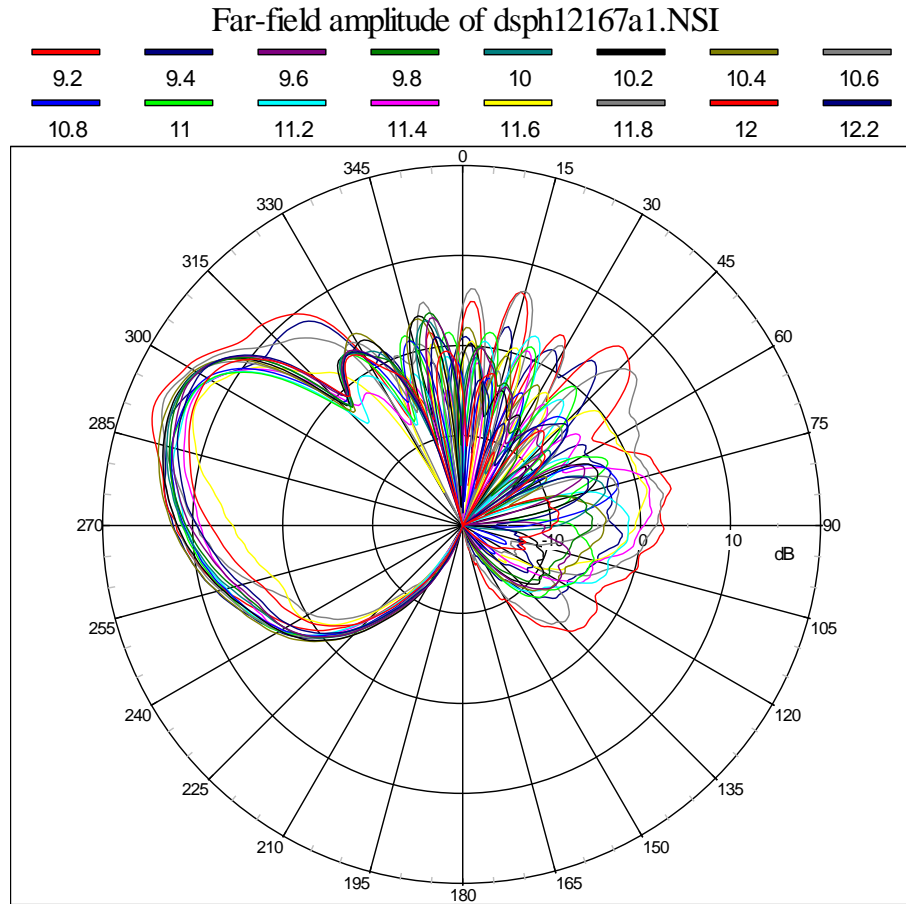


Figure 2.2-4. Measured Elevation Plane Cuts (dBi) from 9.2 to 12.2 GHz in 0.2 GHz steps. All Unused ports have OC Coax. Frequencies below 9.2 GHz not shown since Gain drops off a lot.

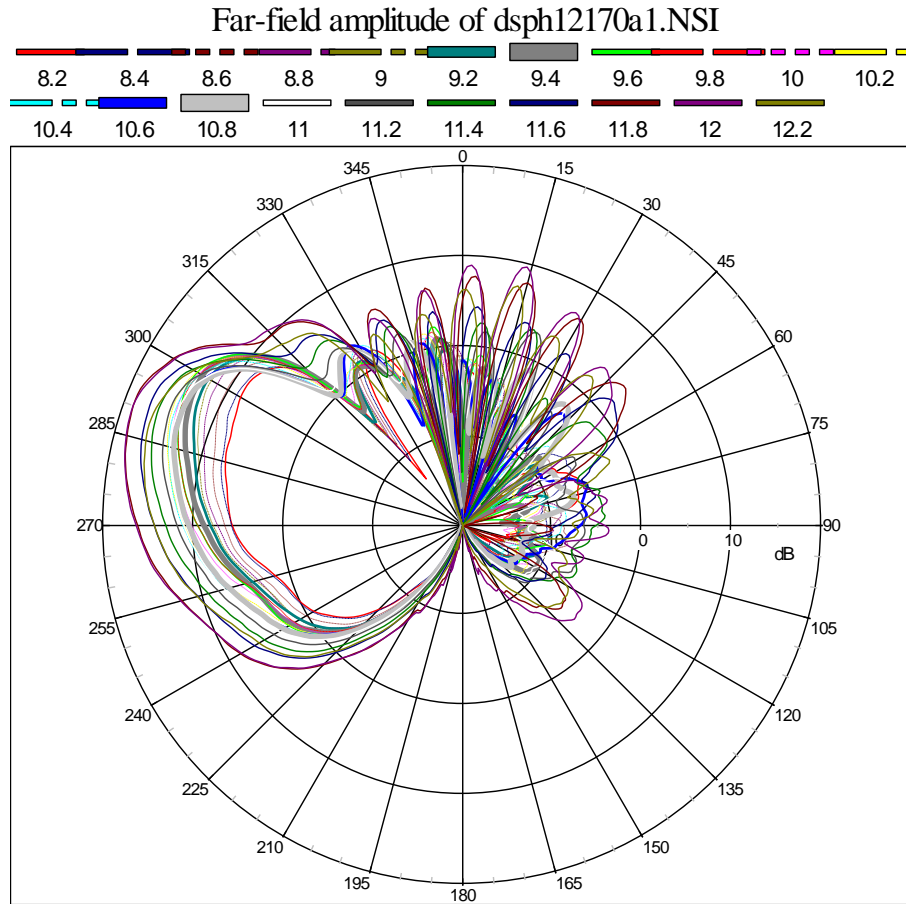


Figure 2.2-5. Measured Elevation Plane Cuts (dBi) from 8.2 to 12.2 GHz in 0.2 GHz steps.
All Unused ports have 50-Ω Termination.

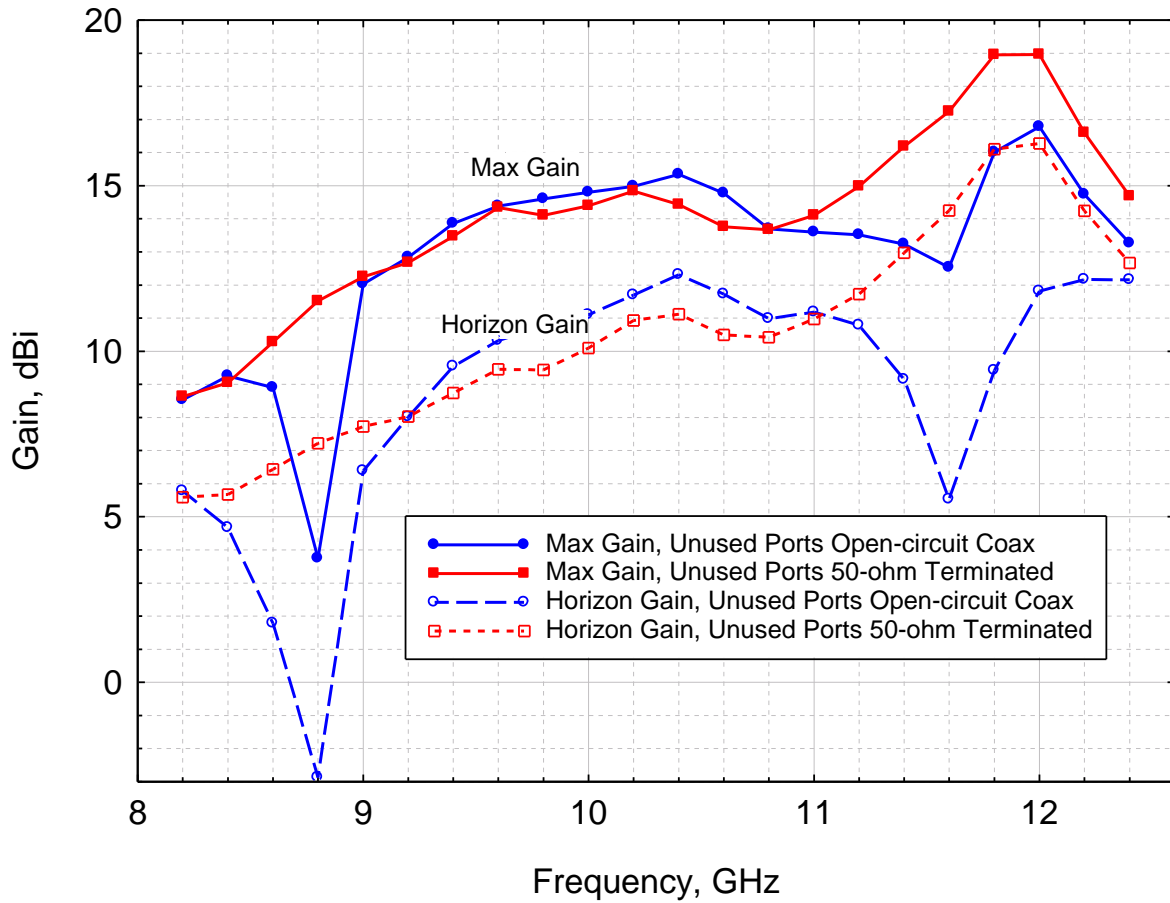


Figure 2.2-6. Measured Gain vs. Frequency, at the Gain Maximum and at the Horizon.

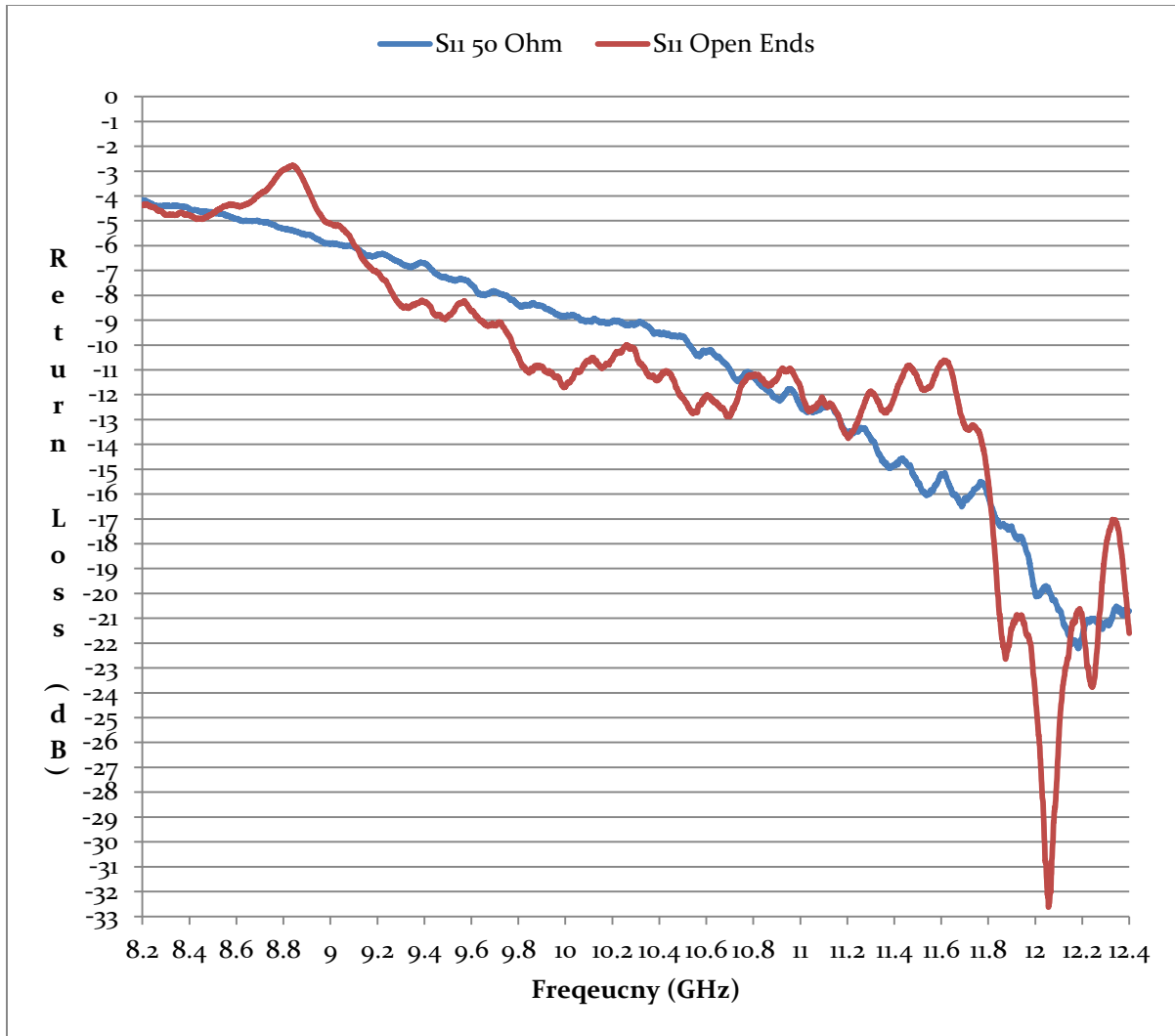


Figure 2.2-7. Measured Return Loss (S₁₁) in dB for One Port. The Other 26 Ports have the OC coax fixtures (blue curve), or the 50 Ω Terminations (red curve).

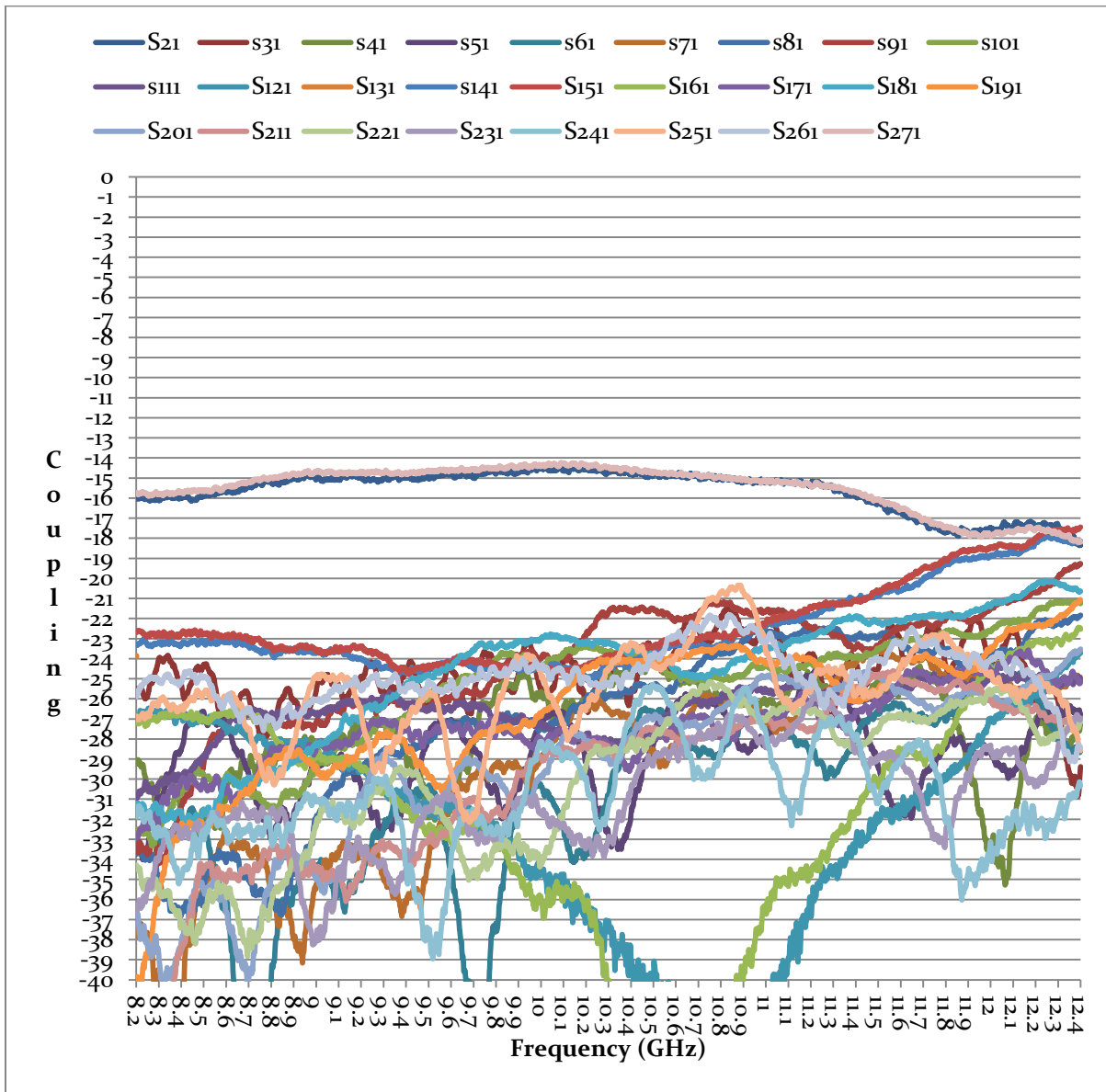


Figure 2.2-8. Measured Mutual Coupling (S_{n1}) in dB from Port #1 to all other Ports. Ports terminated in 50 Ω .

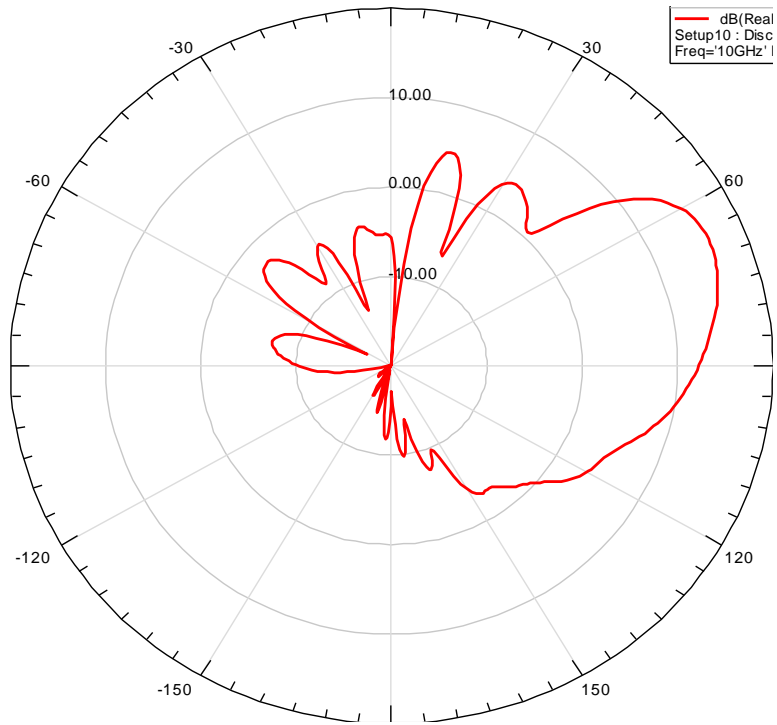


Figure 2.4-1. Computed Elevation Pattern Cut at 10 GHz.

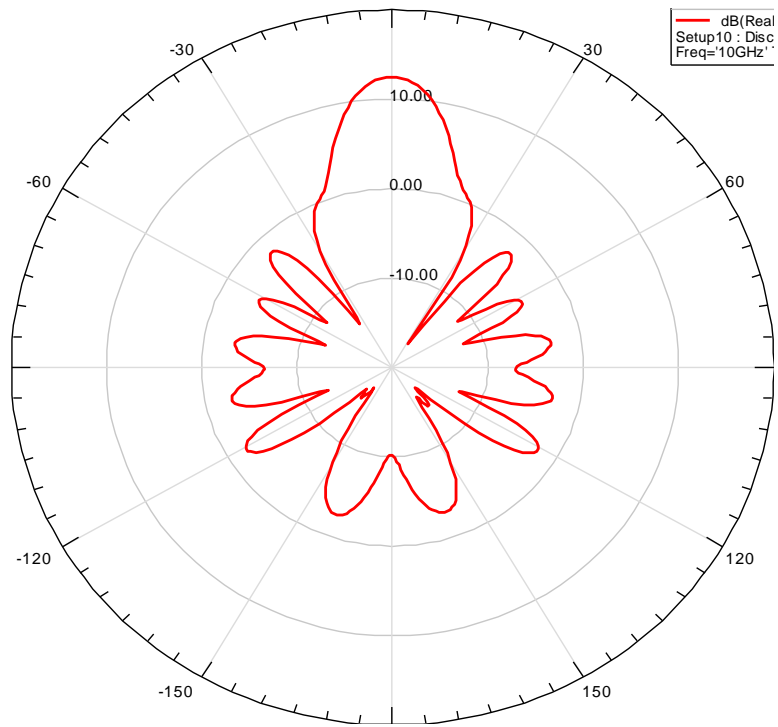


Figure 2.4-2. Computed Azimuth (Horizon) Pattern Cut at 10 GHz.

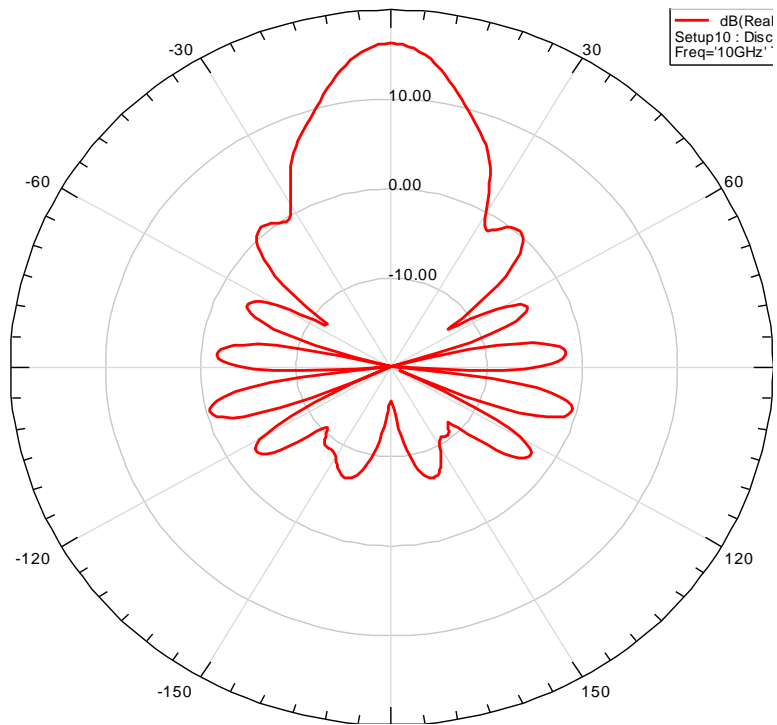


Figure 2.4-3. Computed Conical Pattern Cut at 24° Elevation (i.e. through computed main lobe peak) at 10 GHz.